



OPEN ACCESS

EDITED BY

Heribert Stoiber,
Innsbruck Medical University, Austria

REVIEWED BY

Suresh D. Sharma,
United States Department of Health and
Human Services, United States
Tesfaye Gelanew,
Armauer Hansen Research Institute (AHR),
Ethiopia

*CORRESPONDENCE

Irene M. Ong
✉ irene.ong@wisc.edu

†PRESENT ADDRESSES

Hanying Li,
Xyphos/Astellas, San Francisco, CA,
United States
Richard Pinapati,
Nimble Therapeutics, Madison, WI,
United States
John C. Tan,
Nimble Therapeutics, Madison, WI,
United States

RECEIVED 12 February 2024

ACCEPTED 17 May 2024

PUBLISHED 25 July 2024

CITATION

Vera JM, McIlwain SJ, Fye S, Palmenberg A,
Bochkov YA, Li H, Pinapati R, Tan JC,
Gern JE, Seroogy CM and Ong IM (2024)
Assessing immune factors in maternal
milk and paired infant plasma antibody
binding to human rhinoviruses.
Front. Immunol. 15:1385121.
doi: 10.3389/fimmu.2024.1385121

COPYRIGHT

© 2024 Vera, McIlwain, Fye, Palmenberg,
Bochkov, Li, Pinapati, Tan, Gern, Seroogy and
Ong. This is an open-access article distributed
under the terms of the [Creative Commons
Attribution License \(CC BY\)](#). The use,
distribution or reproduction in other forums
is permitted, provided the original author(s)
and the copyright owner(s) are credited and
that the original publication in this journal is
cited, in accordance with accepted academic
practice. No use, distribution or reproduction
is permitted which does not comply with
these terms.

Assessing immune factors in maternal milk and paired infant plasma antibody binding to human rhinoviruses

Jessica M. Vera^{1,2}, Sean J. McIlwain^{1,2}, Samantha Fye³,
Ann Palmenberg⁴, Yury A. Bochkov³, Hanying Li^{5†},
Richard Pinapati^{5†}, John C. Tan^{5†}, James E. Gern³,
Christine M. Seroogy³ and Irene M. Ong^{1,2,6,7*}

¹Department of Biostatistics and Medical Informatics, University of Wisconsin-Madison, Madison, WI, United States, ²University of Wisconsin Carbone Comprehensive Cancer Center, University of Wisconsin-Madison, Madison, WI, United States, ³Department of Pediatrics, University of Wisconsin-Madison, Madison, WI, United States, ⁴Department of Biochemistry, University of Wisconsin-Madison, Madison, WI, United States, ⁵Roche Nimblegen, Roche Sequencing Solutions, Madison, WI, United States, ⁶Department of Obstetrics and Gynecology, University of Wisconsin-Madison, Madison, WI, United States, ⁷Center for Human Genomics and Precision Medicine, University of Wisconsin-Madison, Madison, WI, United States

Introduction: Before they can produce their own antibodies, newborns are protected from infections by transplacental transfer of maternal IgG antibodies and after birth through breast milk IgA antibodies. Rhinovirus (RV) infections are extremely common in early childhood, and while RV infections often result in only mild upper respiratory illnesses, they can also cause severe lower respiratory illnesses such as bronchiolitis and pneumonia.

Methods: We used high-density peptide arrays to profile infant and maternal antibody reactivity to capsid and full proteome sequences of three human RVs - A16, B52, and C11.

Results: Numerous plasma IgG and breast milk IgA RV epitopes were identified that localized to regions of the RV capsid surface and interior, and also to several non-structural proteins. While most epitopes were bound by both IgG and IgA, there were several instances where isotype-specific and RV-specific binding were observed. We also profiled 62 unique RV-C protein loop sequences characteristic of this species' capsid VP1 protein.

Discussion: Many of the RV-C loop sequences were highly bound by IgG from one-year-old infants, indicating recent or ongoing active infections, or alternatively, a level of cross-reactivity among homologous RV-C sites.

KEYWORDS

rhinovirus, infant immunity, breast milk, respiratory illness, peptide array, immunogenic, antibodies, transplacental antibody transfer

Abbreviations: BM, breast milk; NIm, neutralization immunogen site.

Introduction

Maternally derived antibodies are an important form of humoral immunity for both the developing fetus and postnatal infant. Breast milk (BM) is replete with immunological and bioactive molecules that can supplement and stimulate the developing infant immune system (1–3). Viral respiratory infection is the leading cause of hospitalization and acute health care costs for children under the age of five years (4, 5). However, breastfeeding reduces the risk of upper respiratory infections during infancy (6–9). While the mechanisms of protection conferred by breastmilk (BM) remain largely uncharacterized, IgG and IgA antibodies have been directly implicated in protection against two common respiratory viruses, respiratory syncytial virus (RSV) and human rhinovirus (RV), respectively (10, 11).

RSV and RV infections in children commonly cause mild upper respiratory illnesses but can also cause severe lower respiratory illnesses such as bronchiolitis and pneumonia. Historically, RSV has received more attention for its predilection for causing bronchiolitis in infants. However, RV-A and RV-C species are the most frequent viruses detected in children over one year of age who have wheezing illnesses or exacerbations of asthma (12–16). These findings have spurred interest in characterizing infant and maternal humoral immunity to RVs. While the neutralizing immunogenicity of localized RV-A and RV-B capsid surface sites has been well demonstrated, a complete proteome-wide characterization of regions of RV bound by antibodies, including non-structural proteins, is lacking. Additionally, the overlapping contributions of BM relative to induced infant anti-RV antibodies to overall immunity are unknown.

We and others have developed methods for viral humoral profiling using peptide arrays that allow for expansive examination of antibody reactivity to short, linear peptide fragments (17–24). To better understand how placental transfer and human BM confers protection against viral infections and affects infant immune development, we profiled antibody reactivity from BM, cord blood, and infant plasma samples collected from our ongoing observational birth cohort studies. Both IgA and IgG reactivity was profiled against overlapping linear peptide probes covering the capsid or proteomes of three commonly circulating RV genotypes (A16, B52, and C11) and for 62 putative RV-C-specific VP1 capsid antigens using high-density peptide arrays.

Currently RV vaccines do not exist, however, the development of an RV vaccine could have a major public health impact, especially an RV-C vaccine for high-risk population, such as young children with rs6967330 SNP in CDHR3. The large number of RV serotypes is a major obstacle to vaccine development, however, 25- and 50-valent inactivated RV-A vaccines were shown to induce broadly protective responses in animal models (25) suggesting the feasibility of this approach.

Materials and methods

Human subjects

The participants are from an ongoing prospective observational birth cohort study in rural Wisconsin designed to investigate early

life farm exposure influence on immune development and respiratory allergies and illnesses in children (26). The study was approved by the institutional review boards at the Marshfield Clinic and the University of Wisconsin, and all participants provided informed consent before participating in the study. Infant participants in the ongoing study were born between 2013–2020. Infant participants born between 2013–Jan 2018 were enrolled from rural communities and farms in the vicinity of Marshfield, WI. Starting in February 2018, farm, non-farm, and traditional agrarian families were recruited concurrently at two study sites, the Marshfield Clinic and the LaFarge Medical Clinic (part of Vernon Memorial Healthcare). Written informed consent was obtained by the mother. Study procedures for enrolled participants include inclusion/exclusion criteria, questionnaires, environmental assessments, and samples of blood and breast milk using standardized collection kits and procedures (26).

Peptide microarray design and synthesis

The synthesized arrays included sequences covering the complete proteomes of human rhinoviruses B52, and C11, the capsid polyprotein sequence of RV-A16, and 62 RV-C “C-loop” sequences (27–29). Peptides covering two exogenous viral protein sequences (Epstein-Barr virus (EBV) nuclear antigen 1 and cytomegalovirus (CMV) glycoprotein B) were included as controls. All proteins were tiled as 16 amino acid peptides with a step size of one amino acid. Additional peptides, 15–12 amino acids in length, were tiled at the protein C-terminus to increase coverage of these residues.

The chosen viral peptide sequences were printed onto peptide microarrays (Nimble Therapeutics Madison, Wisconsin, USA) (21) using a Nimble Therapeutics Maskless Array Synthesizer (MAS) and light-directed solid-phase peptide synthesis using an amino-functionalized support (Geiner Bio-One) coupled with a 6-amino-hexanoic acid linker and amino acid derivatives carrying a photosensitive 2-(2-nitrophenyl) propyloxycarbonyl (NPPOC) protection group (Orgentis Chemicals). Peptides with potential sequence overlap were placed in non-adjacent positions on the array to minimize impact of positional bias. Each array consisted of 12 subarrays containing up to 391,551 unique peptide sequences to probe each sample.

Peptide microarray sample assay

Biospecimens were uniformly collected using centralized collection kits and standardized procedures. Plasma samples were obtained from blood collected in sodium heparin tubes (BD 366480), centrifuged for separation of cells and plasma, and plasma was removed and stored at -80°C until use.

Breast milk (BM) was collected at infant’s 2-month study visit. BM samples were thawed on ice and centrifuged (10,000 x g for 10 minutes at 4°C), to separate fat and cells from whey. The fat layer was carefully removed with a sterile spatula and any residual lipids were aspirated using a wide-bore pipette tip. The clear supernatant containing whey and plasma samples were stored at -80°C until use.

IgG binding was assayed as previously described (24). IgA primary sample binding was detected via FITC-conjugated goat anti-human IgA (Jackson ImmunoResearch; RRID: AB_2337652), which was scanned at 488 nm.

Peptide microarray data analysis and visualization

pepMeld (<https://github.com/DABAKER165/pepMeld>) was used to process the raw array fluorescence intensity data as previously described (24). Raw fluorescence signal intensity values were \log_2 transformed, and clusters of fluorescence intensity of statistically unlikely magnitude, indicating array defects, were identified, and removed. Local and large area spatial corrections were then applied, and the median transformed intensity of peptide replicates was determined. The resulting data was cross normalized using quantile normalization. Lastly, probe fluorescence intensity values were smoothed by averaging the signal intensities across a three-probe window centered on each probe. For each sample type, two technical replicates for at least two separate samples were profiled. A Pearson correlation threshold of ≥ 0.73 was used to filter pairs of technical replicates to allow most technical replicates to be retained. The smoothed signal for remaining technical replicates were averaged for each sample before any calls were made concerning epitope probabilities.

Heatmaps representing the array data were created using the ComplexHeatmap version 2.6.2 (30) package in R.

Statistical analysis

Each test sample was profiled for both IgG and IgA reactivity. However, human BM contains predominantly secretory IgA while plasma has much more IgG (31). The observed differences in the antibody reactivity profiles between BM IgA and plasma IgG were consistent with reported differences in the abundances of these two immunoglobulins in these fluids. In addition, BM IgA displayed higher overall signal intensity and lower signal-to-noise ratio compared to plasma IgG. These differences could be due to the compositional differences between plasma and BM, specificity in anti-IgG and anti-IgA secondary antibodies used in our assay, or the overall specific activity of IgA and IgG antibodies. As a result, we processed plasma IgG data and BM IgA data as separate sample populations and defined sample-type specific epitope calling criteria for each.

Sample population mean and standard deviation were used to calculate a z-score for each probe. A z-score threshold of 3 for plasma IgG and 2.5 for BM IgA samples were set to define those probes with statistically significant antibody reactivity. “Epitopes” were defined as consecutive runs sequence-adjacent probes scoring above the z-score threshold in each test sample. Non-consecutive, singleton probes with significant reactivity in only a single test sample were discarded. Statistical analyses were performed in R version 4 using in-house scripts (see Data and code availability).

Protein structures

The virion capsid structures of A16 (1aym), B14 (4rhv), and C15 (5k0u) have been determined to atomic resolution. Residue coordinates were obtained from <https://rcsb.org>. The array-profiled sequences of B52 and C11 are direct homologs to the capsid proteins of B14 and C15 respectively, so the analogous peptides (B52, C11) could be readily identified by sequence alignment and annotated on the known structures (B14, C15). Within the PyMol coordinate display program, the data2bfactor Python script (The PyMOL Molecular Graphics System, Version 2.0 Schrödinger, LLC) was used to substitute numerical parameters representing the peptide array data, replacing each coordinate file’s B-factor column.

RV molecular detection and typing

Nasal swabs collected from participating infants at the indicated surveillance timepoints and during illness episodes were assayed for all common respiratory viruses by multiplex reverse transcription polymerase chain reaction (NxTAG Respiratory Pathogen Panel, Luminex, Austin TX). RV isolates were partially sequenced to identify the species and type and to differentiate lengthy single infections from serial infections with multiple RV strains (32).

RV capsid protein alignments

All RV-A and RV-B share strong capsid structure conservation and readily identifiable sequence homology in key internal protein sub features, making it possible to accurately predict and identify analogous NIm surface locations for equivalent viruses. Analogy-based RV capsid protein sequence alignments were generated as previously described (33).

RV-C VP1 C-loops homologous sequence clusters

Refined C loop multiple sequence alignment and Neighbor-Joining (NJ) tree were created using MUSCLE version 3.8.31 (34). Using the R phylogram package (v 2.1.0) (P. 35) the NJ tree was processed to allow conversion to a hierarchical cluster object and cut into 12 clusters.

Results

Controls for antibody profiling

A newborn’s capacity to mount adaptive immune responses is limited and largely depends on innate and passive immunity for protection against infectious disease. Infant passive immunity is conferred *in utero* via placental transfer of maternal peripheral blood IgG antibodies, and by IgA and IgG antibodies acquired

postnatally via breast milk (BM). By one year of age, transplacental antibodies have typically waned and the maturing infant immune system is the sole source of antibodies, induced thereafter by acquired infections and vaccinations. The landscape of maternally contributed and infant-derived antibodies to three species of RV were profiled for both IgG and IgA reactivity to 275 participant samples, including BM, cord blood, and infant plasma at 1 year of life (Table 1). The cohort was partially concordant, with a total of 54 sets of BM, cord blood, and infant plasma samples from the same mother-infant dyads.

In addition to testing for IgG and IgA reactivity to RV, we also profiled for reactivity to viral antigens from Epstein-Barr virus (EBV) nuclear antigen 1 (P03211) and cytomegalovirus (CMV) glycoprotein B (P06473) (Figure 1). Nearly all adults have antibody reactivity to at least one of these viruses so their antigens provided powerful positive controls, especially for BM (36–41). Indeed, we found all tested BM IgA and cord blood IgG samples showed significant reactivity to at least one of these probes. Infant samples also showed reactivity to these control proteins, however, on average, fewer epitopes were bound and lower signal intensities were observed. For example, infant EBV IgG reactivities were largely confined to the alanine-glycine rich repeats of nuclear antigen 1 (probes ~87-325) and moreover had lower signal intensity compared to maternal (mother-child dyad) cord blood IgG (Supplementary Figure 1A). The IgG reactivity to EBV nuclear antigen 1 peptides among infant samples moderately correlated with cord blood IgG reactivity (median Pearson's $r = 0.66$, $N = 61$).

RV signal differentiation by Ab sample type

BM IgA ("maternal IgA"), cord blood IgG ("maternal IgG"), and 1-year infant IgG samples were assayed for reactivity against a total of 5,294 16-12mer peptides tiling RV A16 capsid proteins (VP1-4) and RV B52 and C11 complete polyproteins (Figure 2; Supplementary Data). Every sample showed statistically significant reactivity to one or more probes for each RV genotype (Supplementary Data). Moreover, as evidenced by the heatmap banding patterns, there was notable similarity in antibody binding calls (Supplementary Figure 2) between different sample types and across all three RV species. When the data were realigned to directly compare analogous sequences, there was even stronger concordance in the most significant sites of epitope calls between A16, B52, and C11 (Pearson's $r = 0.46$ to 0.87), especially for the maternal IgG calls (Supplementary Figure 3B).

It is also evident from the heatmaps that overall, and especially within the densest epitope regions, the maternal cord blood IgG

epitope calls appeared qualitatively stronger compared with BM IgA. In addition, among mother-child dyads, there were more A16 and B52 epitope calls in cord blood compared to the infant samples at 1 year (Supplementary Figure 3). However, infant IgG samples had slightly more C11 calls compared to maternal IgG, possibly due to a greater frequency of RV-C infections among infants (42). Analysis of nasal mucus collected from infants during regular health checkups and self-reported illnesses indicate a significantly higher number of confirmed RV-C infections compared to RV-A ($P = 0.0382$; paired, one-sided Welch's t-test) and RV-B ($P = 1.092 \times 10^{-10}$; paired, one-sided Welch's t-test), among tested infant samples.

Although IgG and IgA epitopes predominately co-localized, we identified 491 probes (from A16, B52, or C11) with disproportionate antibody binding between BM IgA and cord blood IgG samples (proportions test, $FDR < 0.001$) (Supplementary Data). Most of these probes were bound by a greater proportion of BM IgA samples. Notably, a BM IgA-specific epitope was observed near the B52 and C11 VP2 N-terminus (spanning probes 76-83 and 72-83, respectively) and in C11 VP1 (probes 701-707) (Supplementary Figures 4A-C). Cord blood and infant IgG samples disproportionately bound 193 probes, with more infant samples binding to B52 and C11 non-structural protein sites than cord blood IgG. Several B52-specific sites were preferentially bound by cord blood IgG samples, including probes 332-349 (VP3 N-terminus), probes 826-839 (VP1) and 843-853 (VP1); there was little-to-no BM IgA or infant IgG recognition of these B52 epitopes.

Reactivity with known surface neutralization sites

RV virions have 60 identical protein subunits arranged with icosahedral symmetry. Each subunit is derived from a single cleaved polyprotein precursor. The 3 largest proteins, VP1-3, contribute equivalently to the virion surface. A smaller fourth protein (VP4) is packed adjacent to the interior RNA (43). Neutralizing immunogenic sites (NImS), as defined by VP1-3 escape mutations to monoclonal antibodies, have been mapped in cell culture for A2 and B14 isolates. Exclusively confined to the outer virion surfaces, these reported locations generally tag flexible protein surface loops contributed by structurally adjacent sequences. The composite NImS for A2 (sites A, B, C) and for B14 (NIm-I, NIm-II, NIm-III) occupy roughly analogous surface topologies when the respective capsid coordinates are superimposed (Figure 3). The strong conservation among all RV structures, combined with homology-based sequence alignments allow prediction of

TABLE 1 Cohort sample summary.

Sample	Count	Collection Time Point	Maternal Age (years) ^a	Humoral Profile	Antibody
breast milk	108	2 months	30.4 ± 4.2	maternal	IgA
cord blood plasma	93	birth	30.7 ± 4.3	maternal	IgG
infant plasma	74	1 year	31.4 ± 3.9	infant	IgG

^amean age of mother at child's birth ± one standard deviation.

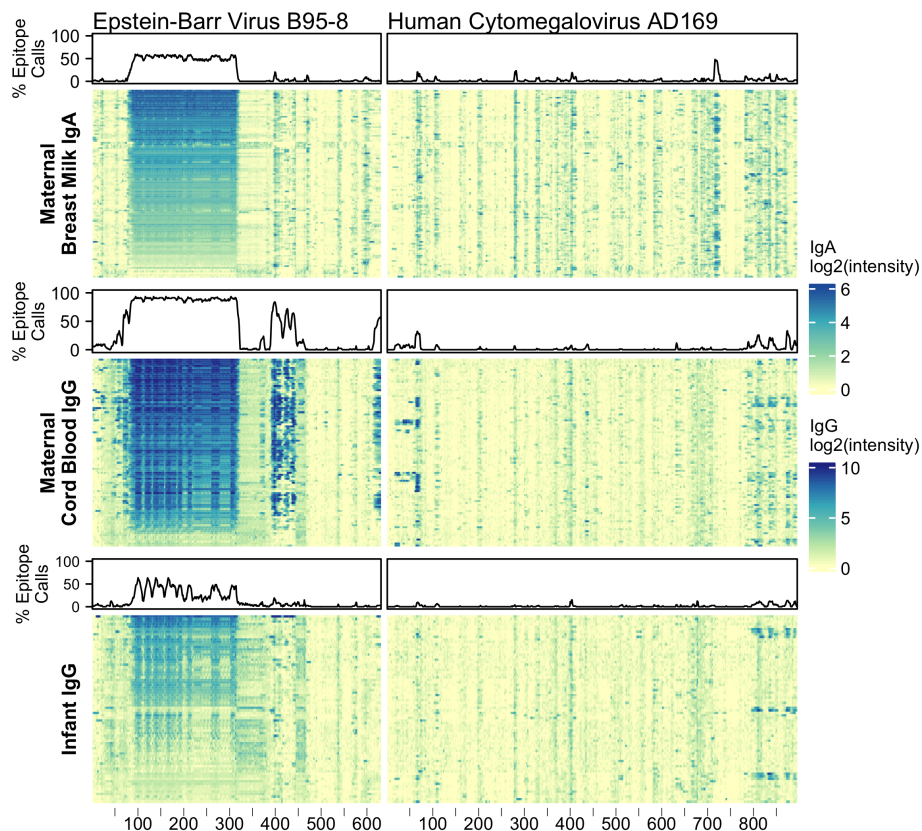


FIGURE 1

Maternal IgA and IgG and infant IgG reactivity to common viral antigen control proteins. Heatmap of antibody reactivity to tiled Epstein-Barr Virus nuclear antigen 1 (P03211) and Cytomegalovirus glycoprotein B (P06473) peptide sequences on a peptide microarray. IgG and IgA sample data were processed as distinct populations. Above each sample population is a line plot indicating the percent of samples with statistically significant reactivity to that probe.

comparable elements for equivalent viruses, especially within the same species. Each A2 NIm surface feature residue has direct homolog in the A16 proteome tiled on the peptide array; the B14 NIm locations, likewise, are predictors of analogous B52 sites (Figure 2, red bars in annotation).

When the A2:A16, B14:B52 sequence and structure equivalents were annotated with observed array calls, reactivity to NIm sites was highly variable, dependent upon the source of the antibody and also on each protein's residue contribution to that site (Table 2).

Reactivity to the annotated A2 NIm sites in A16, varied across sample types and antibody isotypes (Table 2). For example, reactivity to A2:A16 Site A was biased toward cord blood IgG. Here we define bias as a statistically significant difference in the proportion of sample binding. Reactivity to A2:A16 VP3 Site B was biased towards BM IgA. Reactivity to A2:A16 Site C, which includes two regions of VP2, was limited to the C-terminal residues of this NIm site, found in probes 288-305.

As many as 92% of cord blood IgG samples are bound to B14: B52 NIm-IIa and NIm-IIb. The B14 structure configures this region as a continuous VP2 surface sequence with slightly more external exposure than the analogous A16 Site B (VP2) segment. An orthologous VP2 epitope was also observed in A16 and C11 VP2 proteins (Figure 2), which aligns to the B14 NIm-IIa site. Infant IgG reactivity values and epitope binding were highly correlated

between the A16 and B52 B14 NIm-IIA site (Supplementary Figure 5). In A16 the B14 NIm-IIa site is distinct from and located just upstream of the A2 Site B NIm site and prominent A16 epitopes overlap each site. However, reactivity to NIm-IIa and Site B in A16 varied considerably depending on the sample type. While cord blood IgG and BM IgA primarily reacted to NIm-IIa, infant IgG reactivity varied considerably, with each sample reacting to either Site B or NIm-IIa but rarely to both.

In addition to NIm sites, several other capsid peptides have been validated experimentally in animal models as immunogenic, and possibly conserved as epitopes in related picornaviruses (Figure 2, purple bars in annotation). These include two B14 10mer capsid fragments in VP1 and VP2 (43, 44) (Table 2). The Rossmann VP1 peptide was bound consistently across all sample types and RV species. The B52 VP1 Rossmann peptide was bound by the greatest overall proportion of samples and was biased to IgG samples. In contrast, the C11 VP1 peptide was biased to BM IgA.

Reactivity with the capsid interior

Aside from the known external surface virion neutralizing sites (NIm), multiple other capsid segments, in all three RV species, were bound by samples. Among the most prominent sites were

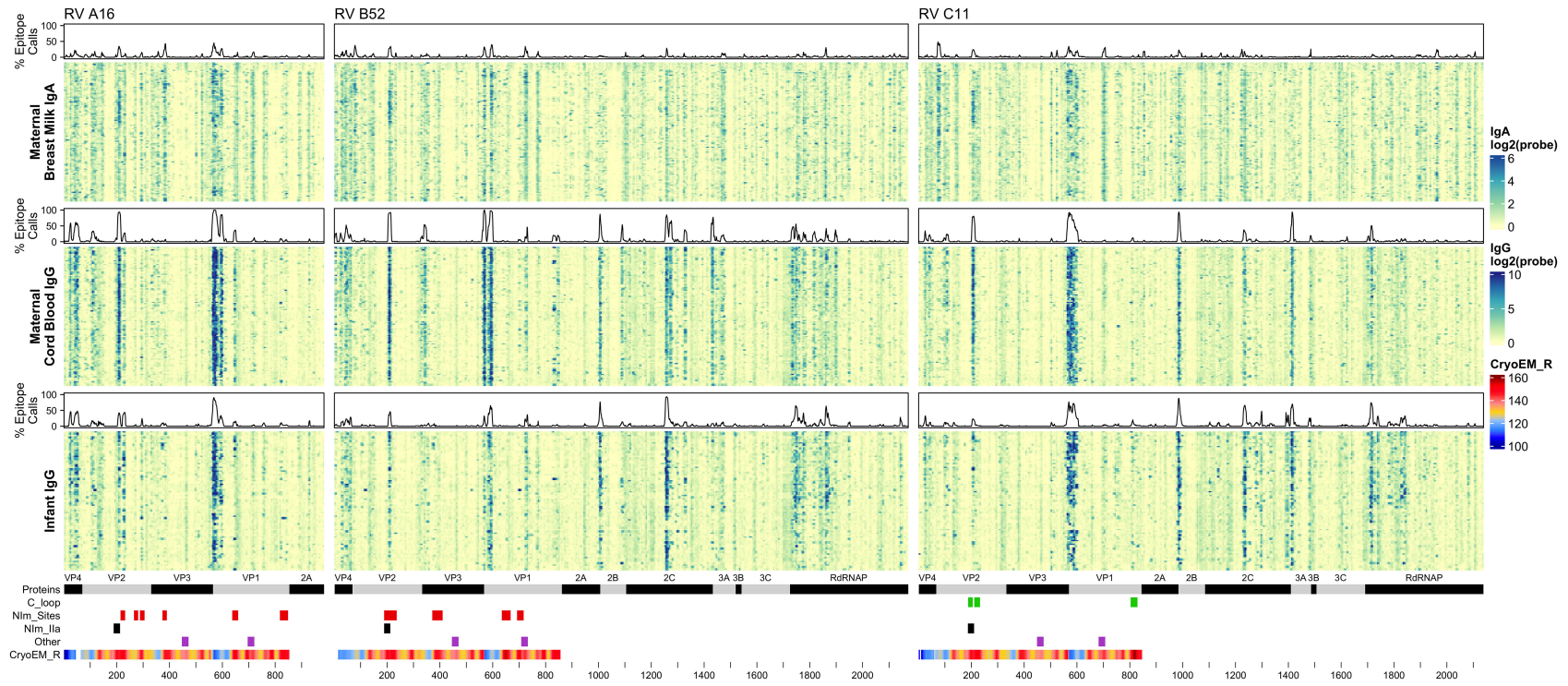
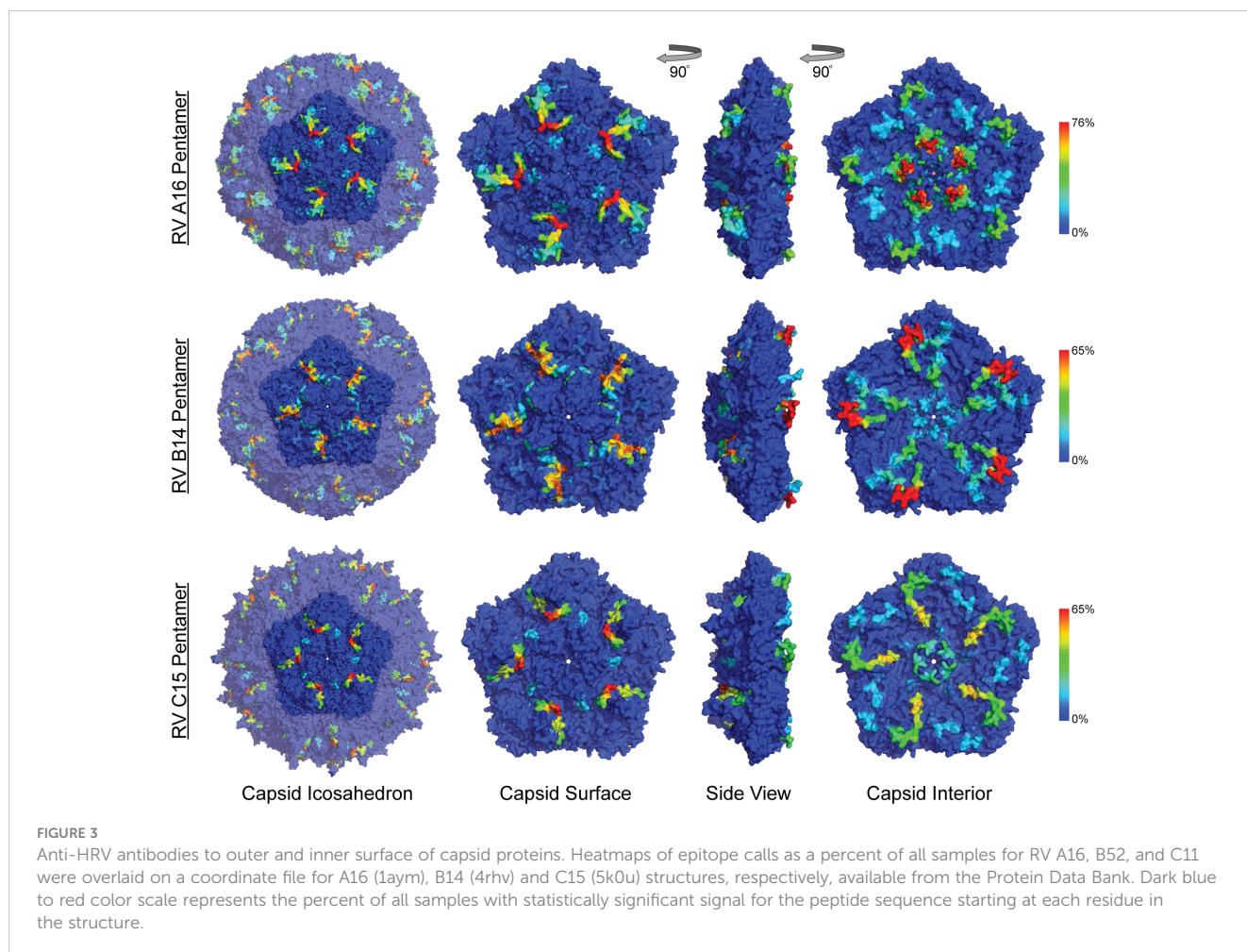


FIGURE 2

Maternal IgA and IgG and infant IgG reactivity to RV (A, B, C) structural and non-structural proteins. Heatmap of antibody reactivity to tiled RV peptide sequences on a microarray. IgG and IgA sample data were processed as distinct populations. Above each sample population is a histogram of the percent of samples with statistically significant reactivity (i.e. epitopes) to that peptide. Several annotations are displayed below the heatmap including mature protein products, RV C C-loop residues (green), RV A2 and B14 NIm sites (red), B52 NIm-Ila sites-specifically (black), experimentally validated immunogenic peptides from (43) (purple), and cryo-EM derived radius values measuring the distance in Angstrom of a given capsid protein residue to the capsid structure center, for each probe the radius value is averaged over the residues of the peptide sequence, those probes with larger average radius values contain residues on the surface of the capsid structure.



peptides spanning the VP3 C-terminus and VP1 N-terminus. In mature virions, the majority of these residues are structurally interior, but when subunits are assembling, they are sequence-adjacent until separated by proteolytic cleavage. The cord blood and infant IgG samples show these regions to be highly bound (Figure 2) consistently displaying as a twin pair of epitopes for A16 and B52, but somewhat more continuous in the analogous region of C11. BM IgA samples had the same patterns, but in fewer samples. Among infant IgG samples though, there was a great deal of preference variability for the upstream (VP3) or downstream (VP1) segment of the pair. The infant IgG samples differentially bound to 90% and 34% of the A16 upstream and downstream segments, respectively, possibly indicating that different physical antibodies bind to these two sites, or that they are not simultaneously exposed during antibody formation or considered contiguous for recognition.

RV non-structural protein epitopes

RV nonstructural proteins are not encapsidated into virions, but they are present in the cytoplasm of infected cells and in airway secretions during illnesses. For completeness, the full proteomes of B52 and C11 were included on the peptide arrays. Several common reactive regions were found, most notably at the 2A protease C-terminus, the

2B N-terminus, the middle of 2C, and in the N-terminal half of the 3D polymerase. As with the capsid samples, reactivity was more pronounced for cord blood and infant IgG. Especially with the infant IgG samples, the C11 banding patterns (Figure 2) were more coherent and pronounced, and involved a greater portion of samples, perhaps indicating that certain discrete segments make especially viable epitopes within 2C and 3D, or even within 3A, 3B, and 3C.

Reactivity with RV-C specific VP1 surface loop

RV-C capsids are topologically distinct from the RV-A and RV-B and have never been mapped experimentally for neutralizing NIMs. Species-specific deletions, clearly apparent in the aligned sequences, truncate several VP1 loops contributing to the five-fold region, and consequently remove the NIm-Ia and NIm-Ib homologs that would otherwise be immunogenic (13, 45). Analogs to NIm-II and NIm-III are still surface exposed, but unique to each RV-C subunit, and centered within it, are a pair of species-specific adjacent exposed protein loops contributed by a VP1 C-terminal extension (residues 256-265 RV C15), and nearby VP2 residues (46). The VP1 portion of this “finger” or “C-loop” varies in length (16-23 residues), with up to 70% amino acid

TABLE 2 RV capsid neutralization site reactivity

RV	Site	Protein	Probes	IgA Breast Milk (%)	IgG Cord Blood (%)	IgG Infant (%)	Significant Hits ^a
A16	Site_A	VP1	638-659	15.7	36.6	16.2	647,648,649
	Site_B	VP1	818-848	5.6	9.7	10.8	
	Site_B	VP2	215-231	16.7	58.1	43.2	
	Site_B	VP3	374-389	42.6	8.6	10.8	384,385
	Site_C	VP2	266-281	5.6	4.3	5.4	
	Site_C	VP2	288-305	15.7	8.6	24.3	
	Rossmann A16	VP3	447-471	0	1.1	2.7	
	Rossmann A16	VP1	696-720	16.7	12.9	4.1	
	B14 NIm-IIa	VP2	189-212	34.3	93.5	41.9	208,211
B52	NIm-IIa	VP2	189-212	32.4	91.4	45.9	209,211,212
	NIm-IIb	VP2	209-236	34.3	92.5	45.9	209,211-213
	NIm-IIIa	VP3	371-395	2.8	2.2	8.1	
	NIm-IIIb	VP3	387-410	9.3	1.1	1.4	
	NIm-Iab	VP1	635-667	4.6	3.2	1.4	
	NIm-Ia	VP1	692-716	4.6	6.5	5.4	
	Rossmann B52	VP3	446-470	3.7	0	2.7	
	Rossmann B52	VP1	708-732	34.3	46.2	36.5	730
C11	C loop	VP2	188-205	21.3	78.5	21.6	204,205
	C loop	VP2	212-232	14.8	62.4	16.2	212
	C loop	VP1	803-828	5.6	12.9	20.3	
	Rossmann C11	VP3	449-473	3.7	0	0	
	Rossmann C11	VP1	682-706	31.5	5.4	5.4	705,706
	B14 NIm-IIa	VP2	187-210	24.1	80.6	23	204-206,208

^aprobe IDs with three-sample proportions test adjusted p-val < 0.01.

diversity (average 50%) among the 57 recognized RV-C types. The C-loop is hypothesized to function as a dominant neutralization site, an apparent structural substitute for the missing NIm-Iab (46). The contributing VP2 residues (136-138;160-165) at the base of the C-loop partially align to the B14 NIm-IIa site, further supporting the likely immunogenicity of this unique RV-C feature (Figure 2).

Approximately 40% of all tested samples showed significant binding to C11 VP2 C-loop residues (Table 2), particularly in cord blood IgG samples. Only 6-20% of the combined samples showed reactivity to the more prominent C11 VP1 loop component. This was slightly more common among the infant IgG samples. Our accompanying viral diagnostics that followed these infants indicated only about 4% ever had a confirmed RV-C11 infection during their first year of life which is considerably fewer than those exhibiting reactivity to the C11 C-loop. While sparsity within our nasal swab PCR data is a likely contributor to this incongruity, it raised the possibility that RV cross-reactivity, at this or other prominent epitope sites, might contribute to the observed signals.

A potential test for cross-reactivity was embedded within our array design by the inclusion of 16mer peptides tiling VP1 C-loop from 57 RV-C and five putative RV-C genotype sequences (Figure 4). The largest proportion of infant IgG samples (57%) bound to C33 and C17 VP1 C loop segments. In contrast, no tested infant samples bound to C42 (JF416320), even though as many as 24% of infant samples showed reactivity to a related C42 sequence (JQ994500). This pair of isolates differs by 6 (of 16) amino acids over the sampled region, a diversity that is typical for other RV-C pairs in the C-loop region.

Since cross-reactivity likely depends on sequence diversity, the infant IgG data were reparsed according to a C-loop Neighbor-Joining tree. The phylogram closely resembled published RV-C trees based on complete VP1 or VP0 sequences (47, 48), and identified at least three groups of infant samples with distinct preference for homologous C-loop sequence clusters. Sample group 1 (N = 7) had predominant reactivity to C-loop cluster 12, sample group 3 (N = 8) had reactivity to subsets of C-loop clusters 8 and 12, while sample

group 2 (N = 59) consisted of samples with limited or overall reduced C-loop reactivity. These results did not change when redundant probe sequences (i.e., probes common to more than 1 virus) were removed (data not shown) indicating that positive calls were not due to artefactually similar C-loop probe sequences. Within infant cluster 1, for example, there was an observed enrichment for C6 infections ($P = 0.027$; hypergeometric test), but no enrichment for other RV. Not only did several of these IgG samples bind the C6 probes they also bound those C-loops most related to C6. As with the C11 data cited above, this again indicates the potential for cross-reactivity, at least for this epitope, within this phylogenetic group.

Discussion

We profiled the IgG and IgA antibody binding landscapes of mother and infant samples against three rhinovirus species. This is the first proteome-wide examination of RV B-cell epitopes comparing maternal (cord, BM) transfer of IgG and IgA antibodies via placenta and breastmilk respectively, to the fetus and newborn, offering passive protection until infants develop active antibody responses to infection (1 year plasma). We also profiled reactivity to the prominent RV-C C-loop structures that were predicted to be highly immunogenic. Highly immunogenic epitopes displayed a striking degree of concordance across sample types, antibody isotypes, and RV types. RV- and antibody isotype-specific epitopes were identified for capsid and non-structural proteins. Many less common epitopes were also present (found in <10% of samples for a given sample type) that may represent private B cell receptor repertoires or possibly cross-reactivity from infection from heterotypic RVs.

By profiling cord and BM samples these experiments produced new information about the quantity and particular anti-RV antibodies that the placenta and breastmilk transfers to the infant in the form of IgG and secretory IgA. Breastfeeding reduces respiratory illnesses (49), but little is known about how BM antibodies protect against RV. One study observed that RV neutralization by BM was dependent on sIgA (10). For RSV, BM IgG neutralizing antibody titer was a strong correlate of immunity for infant RSV infections (11). We observed a high degree of concordance between maternal RV epitopes from plasma IgG and BM IgA, including epitopes at known NIm sites, which may protect against RV infections in early infancy. We also observed BM IgA-specific epitopes on the virion interior and surface of B52 and C11.

RV NIm sites are structural antibody epitopes composed of residues brought in close proximity by protein folding and capsid assembly. Our array was composed of short, linear, unmodified peptides which does not replicate higher orders of protein structure, nor does it account for post-translational modifications that may be integral to antibody recognition. Nonetheless, samples reacted strongly to array peptides spanning VP2, and to a lesser extent VP1 NIm sites. Others have also reported strong IgG reactivity to short linear peptides spanning the A16 NIm-II site (50). The absence of reactivity at other NIm sites may indicate a greater dependence on the capsid protein structure or protein modifications for antibody reactivity to these sites. NIm site

reactivity may also require seroconversion from homotypic RV infection. The nearly ubiquitous reactivity to VP2 NIm sites suggests that these sites are not only less dependent on the capsid conformational structure but may also be highly cross-reactive.

Neutralization sites have not been characterized for RV-C. Our infant and maternal samples reacted to several C11 virion surface features, including the VP1 and VP2 flexible protein loop protrusion ("C-loop"). Examination of additional RV-C C-loop sequences demonstrated strong reactivity, especially from infant samples, and further investigation is warranted to determine if C-loops are RVC NIm sites. Despite the considerable sequence diversity of RV-C C-loops, we observed evidence of putative cross-reactivity at these sites based on similar reactivity patterns between homologous C loops sequences. A recent study reported reciprocal cross-reactive neutralization between RV C2 and C40 in both mouse and human samples (51). Our findings also grouped together RV C2 and C47 C-loops as putative cross-reactive epitopes indicating that potential cross-reactivity patterns can be deconvoluted from antibody binding profiles collected from peptide microarrays.

Numerous IgG and IgA epitopes localized to the virion surface and interior and to non-structural proteins. These potentially novel surface epitopes may represent additional neutralization sites, non-neutralizing antibody-dependent protection sites that aid in viral clearance (52), or sites for intracellular inhibition of viral replication and assembly (53). One of the most striking and immunodominant epitopes observed, spanning the VP3 C-terminus and VP1 N-terminus, consists of residues largely internal to the RV capsid structure. A previous study also observed IgG1 and IgM reactivity to RV VP1 N-terminal peptides that do not contain surface exposed residues (54). Interestingly, studies of poliovirus and other enteroviruses related to RV have also reported B cell epitopes within the VP1 N-terminus that localize to the virion interior (55–57). This poliovirus N-terminal VP1 epitope has been characterized as a "T-B epitope pair" by which this B cell epitope also shows strong T cell reactivity thus leading to B cell activation. Several RV-A and C VP1 peptides can stimulate T-cell proliferation in humans suggesting that a VP1 immunogenic T-B epitope pair is conserved across enteroviruses (57, 58). For B-cell epitopes not residing on the virion surface, it is unclear what role they play in mediating the host immune response. Some have proposed this VP1 epitope may act to misdirect the host immune response towards non-neutralizing sites, thus aiding viral escape. How B-cell receptors encounter these "internal" epitopes is unclear. Possibilities include changes in capsid structure during host cell attachment (59), spontaneous capsid conformational changes (aka "breathing") (60, 61), and viral protein release following cell lysis.

Our profiling of peptide-level antibody reactivity to three RV types strongly supports the existence of cross-reactive RV epitopes. Many past and recent studies have reported observations of RV cross-reactivity, which can be examined comprehensively using array technology. Given the abundance and diversity of RV types, high-throughput profiling of RV B-cell epitopes by peptide arrays, as demonstrated here, can identify pan-RV epitopes that may direct the development of improved RV diagnostics, vaccines, and therapeutics.

Data availability statement

The original contributions presented in the study can be found in the article/[Supplementary Material](#). pepMeld-processed and quantile normalized data for all proteins discussed in this paper can be found at Zenodo under the digital object identifier 10.5281/zenodo.8269759. The code used for determining antibody binding from publicly available data set is available at http://github.com/Ong-Research/WISC_WFS_Rhinovirus.

Ethics statement

The studies involving humans were approved by Institutional review boards at the Marshfield Clinic and the University of Wisconsin. The studies were conducted in accordance with the local legislation and institutional requirements. Written informed consent for participation in this study was provided by the participants' legal guardians/next of kin.

Author contributions

JV: Investigation, Methodology, Visualization, Writing – review & editing, Data curation, Formal analysis, Software, Writing – original draft. SM: Investigation, Methodology, Writing – review & editing, Data curation, Formal analysis, Software. SF: Writing – review & editing, Methodology. AP: Investigation, Methodology, Visualization, Writing – review & editing, Data curation. YB: Data curation, Writing – review & editing. HL: Writing – review & editing. RP: Writing – review & editing. JT: Methodology, Writing – review & editing. JG: Funding acquisition, Investigation, Writing – review & editing. CS: Conceptualization, Investigation, Resources, Writing – review & editing. IO: Conceptualization, Funding acquisition, Investigation, Methodology, Project administration, Supervision, Visualization, Writing – original draft, Writing – review & editing.

Funding

The author(s) declare financial support was received for the research, authorship, and/or publication of this article. IO acknowledges support by the Clinical and Translational Science Award (CTSA) program (ncats.nih.gov/ctsa), through the National Institutes of Health National Center for Advancing Translational Sciences (NCATS), grants UL1TR002373 and KL2TR002374, support through National Institutes of Health National Institute of Allergy and Infectious Diseases grant 2U19AI104317-06 (to IO, JV, and SM via JG and CS), the Data Science Initiative (research.wisc.edu/funding/data-science-initiative/) grant from the University of Wisconsin-Madison Office of the Chancellor and the Vice Chancellor for Research and Graduate Education (with funding from the Wisconsin Alumni Research Foundation, and startup funds through the University of Wisconsin Department of Obstetrics and Gynecology (www.obgyn.wisc.edu/)). This research was also supported by the National Institutes of Health National Institute of Allergy and

Infectious Diseases (www.niaid.nih.gov) grant R01AI148707 to YB. JV, IO, and SM acknowledges support by the National Cancer Institute, National Institutes of Health and University of Wisconsin Carbone Comprehensive Cancer Center's Cancer Informatics Shared Resource (grant P30-CA-14520; (cancer.wisc.edu/research/)). The funders had no role in study design, data collection and analysis, decision to publish, or preparation of the manuscript.

Acknowledgments

We thank the study families for their participation in this study. The authors are grateful to Dr. Deborah Chasman and Dr. Aubrey Barnard for their thoughtful comments and helpful discussions in preparing this manuscript.

Conflict of interest

JG is a paid consultant for AsthmaZeneca, Meissa Vaccines Inc., Via Nova Therapeutics, and Arrowhead Pharmaceuticals and has stock options in Meissa Vaccines Inc. Authors HL, RP, JT were employed by Roche Nimblegen when the work was performed. The companies listed had no role in the design, execution, interpretation, or funding of this research.

The remaining authors declare that the research was conducted in the absence of any commercial or financial relationships that could be construed as a potential conflict of interest.

Publisher's note

All claims expressed in this article are solely those of the authors and do not necessarily represent those of their affiliated organizations, or those of the publisher, the editors and the reviewers. Any product that may be evaluated in this article, or claim that may be made by its manufacturer, is not guaranteed or endorsed by the publisher.

Supplementary material

The Supplementary Material for this article can be found online at: <https://www.frontiersin.org/articles/10.3389/fimmu.2024.1385121/full#supplementary-material>

SUPPLEMENTARY TABLE 1

Genbank and Uniprot accessions for protein sequences tiled on array.

SUPPLEMENTARY TABLE 2

Breast milk IgA epitopes per sample.

SUPPLEMENTARY TABLE 3

Plasma IgG epitopes per sample.

SUPPLEMENTARY TABLE 4

Sample metadata.

SUPPLEMENTARY TABLE 5

Specimen type epitope histogram.

References

- Lawrence RM, Pane CA. Human breast milk: current concepts of immunology and infectious diseases. *Curr Problems Pediatr Adolesc Health Care*. (2007) 37:7–365. doi: 10.1016/j.cped.2006.10.002
- Chirico G, Marzollo R, Cortinovis S, Fonte C, Gasparoni A. Antiinfective properties of human milk. *J Nutr*. (2008) 138:1801S–1806S. doi: 10.1093/jn/138.9.1801S
- Kim YJ. Immunomodulatory effects of human colostrum and milk. *Pediatr Gastroenterology Hepatol Nutr*. (2021) 24:337. doi: 10.5223/pghn.2021.24.4.337
- Witt WP, Weiss AJ, Elixhauser A. Overview of Hospital Stays for Children in the United States 2012. In: *Healthcare Cost and Utilization Project (HCUP) Statistical Briefs*. Agency for Healthcare Research and Quality (US, Rockville (MD) (2006). Available at: <http://www.ncbi.nlm.nih.gov/books/NBK274247/>.
- Duan KI, Birger M, Au DH, Spece LJ, Feemster LC, Dieleman JL. Health care spending on respiratory diseases in the United States 1996–2016. *Am J Respir Crit Care Med*. (2023) 207:183–925. doi: 10.1164/rccm.202202-0294OC
- López-Alarcón M, Villalpando S, Fajardo A. Breast-feeding lowers the frequency and duration of acute respiratory infection and diarrhea in infants under six months of age. *J Nutr*. (1997) 127:436–5. doi: 10.1093/jn/127.3.436
- Bachrach VRG, Schwarz E, Bachrach LR. Breastfeeding and the risk of hospitalization for respiratory disease in infancy: A meta-analysis. *Arch Pediatr Adolesc Med*. (2003) 157:2375. doi: 10.1001/archpedi.157.3.2375
- Jenkins AL, Gyorkos TW, Joseph L, Culman KN, Ward BJ, Pekeles GS, et al. Risk factors for hospitalization and infection in Canadian Inuit infants over the first year of life - a pilot study. *Int J Circumpolar Health*. (2004) 63:61–705. doi: 10.3402/ijch.v63i1.17649
- Sadeharju K, Knip M, Virtanen SM, Savilahti E, Tauriainen S, Koskela P, et al. Maternal antibodies in breast milk protect the child from enterovirus infections. *Pediatrics*. (2007) 119:941–465. doi: 10.1542/peds.2006-0780
- May JT, Clarke NM. Effect of antimicrobial factors in human milk on rhinoviruses and milk-borne cytomegalovirus *in vitro*. *J Med Microbiol*. (2000) 49:719–23. doi: 10.1099/0022-1317-49-8-719
- Mazur NI, Horsley NM, Englund JA, Nederend M, Magaret A, Kumar A, et al. Breast milk preflusion F immunoglobulin G as a correlate of protection against respiratory syncytial virus acute respiratory illness. *J Infect Dis*. (2018) 219:59–67. doi: 10.1093/infdis/jiy477
- Miller EK, Lu X, Erdman DD, Poehling KA, Zhu Y, Griffin MR, et al. Rhinovirus-associated hospitalizations in young children. *J Infect Dis*. (2007) 195:773–81. doi: 10.1086/511821
- Lau SKP, Yip CCY, Lin AWC, Lee RA, So L-Y, Lau Y-L, et al. Clinical and molecular epidemiology of human rhinovirus C in children and adults in Hong Kong reveals a possible distinct human rhinovirus C subgroup. *J Infect Dis*. (2009) 200:1096–11035. doi: 10.1086/605697
- Lee W-M, Lemanske RF, Evans MD, Vang F, Pappas T, Gangnon R, et al. Human rhinovirus species and season of infection determine illness severity. *Am J Respir Crit Care Med*. (2012) 186:886–915. doi: 10.1164/rccm.201202-0330OC
- Han M, Rajput C, Hershenson MB. Rhinovirus attributes that contribute to asthma development. *Immunol Allergy Clinics North America*. (2019) 39:345–595. doi: 10.1016/j.iac.2019.03.004
- Biagi C, Rocca A, Poletti G, Fabi M, Lanari M. Rhinovirus infection in children with acute bronchiolitis and its impact on recurrent wheezing and asthma development. *Microorganisms*. (2020) 8:16205. doi: 10.3390/microorganisms8101620
- Asano A, Torigoe D, Sasaki N, Agui T. Identification of antigenic peptides derived from B-cell epitopes of nucleocapsid protein of mouse hepatitis virus for serological diagnosis. *J Virological Methods*. (2011) 177:107–15. doi: 10.1016/j.jviromet.2011.07.006
- Kuivanen S, Hepojoki J, Vene S, Vaheri A, Vapalahti O. Identification of linear human B-cell epitopes of tick-borne encephalitis virus. *Virology*. (2014) 461:1155. doi: 10.1016/j.virol.2014.11.115
- Stephenson KE, Neubauer GH, Reimer U, Pawlowski N, Knaute T, Zerweck J, et al. Quantification of the epitope diversity of HIV-1-specific binding antibodies by peptide microarrays for global HIV-1 vaccine development. *J Immunol Methods*. (2015) 416:105–23. doi: 10.1016/j.jim.2014.11.006
- Sabalza M, Barber CA, Abrams WR, Montagna R, Malamud D. Zika virus specific diagnostic epitope discovery. *J Visualized Experiments*. (2017) 130:56784. doi: 10.3791/56784
- Heffron AS, Mohr EL, Baker D, Haj AK, Buechler CR, Bailey A, et al. Antibody responses to zika virus proteins in pregnant and non-pregnant macaques. *PLoS Negl Trop Dis*. (2018) 12:e0006903. doi: 10.1371/journal.pntd.0006903
- Zhang H, Song Z, Yu H, Zhang X, Xu S, Li Z, et al. Genome-wide linear B-cell epitopes of enterovirus 71 in a hand, foot and mouth disease (HFMD) population. *J Clin Virol*. (2018) 105:41–8. doi: 10.1016/j.jcv.2018.06.001
- Farrera-Soler L, Daguier J-P, Barluenga S, Vadas O, Cohen P, Pagano S, et al. Identification of immunodominant linear epitopes from SARS-CoV-2 patient plasma. *PLoS One*. (2020) 15:e02380895. doi: 10.1371/journal.pone.0238089
- Heffron AS, McIlwain SJ, Amjadi MF, Baker DA, Khullar S, Armbrust T, et al. The landscape of antibody binding in SARS-CoV-2 infection. *PLoS Biol*. (2021) 19:e3001265. doi: 10.1371/journal.pbio.3001265
- Lee S, Nguyen MT, Currier MG, Jenkins JB, Strobert EA, Kajon AE, et al. A polyvalent inactivated rhinovirus vaccine is broadly immunogenic in rhesus macaques. *Nat Commun*. (2016) 7:12838. doi: 10.1038/ncomms12838
- Seroogy CM, VanWormer JJ, Olson BF, Evans MD, Johnson T, Cole D, et al. Respiratory health, allergies, and the farm environment: design, methods and enrollment in the observational Wisconsin infant study cohort (WISC): A research proposal. *BMC Res Notes*. (2019) 12:423. doi: 10.1186/s13104-019-4448-0
- Tapparel C, Junier T, Gerlach D, Belle SV, Turin L, Cordey S, et al. New respiratory enterovirus and recombinant rhinoviruses among circulating picornaviruses. *Emerging Infect Dis*. (2009) 15:719–26. doi: 10.3201/eid1508.081286
- Nakagome K, Bochkov YA, Ashraf S, Brockman-Schneider RA, Evans MD, Pasic TR, et al. Effects of rhinovirus species on viral replication and cytokine production. *J Allergy Clin Immunol*. (2014) 134:332–3415.e10. doi: 10.1016/j.jaci.2014.01.029
- Gern JE, Lee WM, Swenson CA, Nakagome K, Lee I, Wolff M, et al. Development of a rhinovirus inoculum using a reverse genetics approach. *J Infect Dis*. (2019) 220:187–94. doi: 10.1093/infdis/jiy629
- Gu Z, Eils R, Schlesner M. Complex heatmaps reveal patterns and correlations in multidimensional genomic data. *Bioinformatics*. (2016) 32:2847–495. doi: 10.1093/bioinformatics/btw313
- Hurley WL, Theil PK. Perspectives on immunoglobulins in colostrum and milk. *Nutrients*. (2011) 3:442–745. doi: 10.3390/nu3040442
- Bochkov YA, Grindle K, Vang F, Evans MD, Gern JE. Improved molecular typing assay for rhinovirus species A, B and C. *J Clin Microbiol*. (2014) 52:2461–715. doi: 10.1128/JCM.00075-14
- Palmenberg AC, Spiro D, Kuzmickas R, Wang S, Djikeng A, Rathe JA, et al. Sequencing and analyses of all known human rhinovirus genomes reveal structure and evolution. *Science*. (2009) 324:55–9. doi: 10.1126/science.1165557
- Edgar RC. MUSCLE: multiple sequence alignment with high accuracy and high throughput. *Nucleic Acids Res*. (2004) 32:1792–97. doi: 10.1093/nar/gkh340
- Wilkinson SP, Davy SK. Phylogram: an R package for phylogenetic analysis with nested lists. *J Open Source Software*. (2018) 3:7905. doi: 10.21105/joss.00790
- Dillner J, Sternäs L, Kallin B, Alexander H, Ehlin-Henriksson B, Jörnvall H, et al. Antibodies against a synthetic peptide identify the Epstein-Barr virus-determined nuclear antigen. *Proc Natl Acad Sci*. (1984) 81:4652–56. doi: 10.1073/pnas.81.15.4652
- Rumpold H, Rhodes GH, Bloch PL, Carson DA, Vaughan JH. The glycine-alanine repeating region is the major epitope of the Epstein-Barr nuclear antigen-1 (EBNA-1). *J Immunol*. (1987) 138:593–99. doi: 10.4049/jimmunol.138.2.593
- Meyer H, Masuho Y, Mach M. The gp116 of the gp58/116 complex of human cytomegalovirus represents the amino-terminal part of the precursor molecule and contains a neutralizing epitope. *J Gen Virol*. (1990) 71:2443–50. doi: 10.1099/0022-1317-71-10-2443
- Cheng HM, Foong YT, Sam CK, Prasad U, Dillner J. Epstein-Barr virus nuclear antigen 1 linear epitopes that are reactive with immunoglobulin A (IgA) or IgG in sera from nasopharyngeal carcinoma patients or from healthy donors. *J Clin Microbiol*. (1991) 29:2180–86. doi: 10.1128/jcm.29.10.2180-2186.1991
- Kniess N, Mach M, Fay J, Britt WJ. Distribution of linear antigenic sites on glycoprotein gp55 of human cytomegalovirus. *J Virol*. (1991) 65:138–46. doi: 10.1128/JVI.65.1.138-146.1991
- Ruprecht K, Wunderlich B, Gieß René, Meyer P, Loebel M, Lenz K, et al. Multiple Sclerosis: The Elevated Antibody Response to Epstein-Barr Virus Primarily Targets, but Is Not Confined to, the Glycine-Alanine Repeat of Epstein-Barr Nuclear Antigen-1. *J Neuroimmunology*. (2014) 272:56–61. doi: 10.1016/j.jneuroim.2014.04.005
- Choi T, Devries M, Bacharier LB, Busse W, Camargo CA, Cohen R, et al. Enhanced neutralizing antibody responses to rhinovirus C and age-dependent patterns of infection. *Am J Respir Crit Care Med*. (2021) 203:822–30. doi: 10.1164/rccm.202010-3753OC
- Rossmann MG, Arnold E, Erickson JW, Frankenberger EA, Griffith JP, Hecht Hans-Jürgen, et al. Structure of a human common cold virus and functional relationship to other picornaviruses. *Nature*. (1985) 317:145–53. doi: 10.1038/317145a0
- McCray J, Werner G. Different rhinovirus serotypes neutralized by antipeptide antibodies. *Nature*. (1987) 329:736–38. doi: 10.1038/329736a0
- Basta HA, Sgro J-Y, Palmenberg AC. Modeling of the human rhinovirus C capsid suggests a novel topography with insights on receptor preference and immunogenicity. *Virology*. (2014) 448:176–84. doi: 10.1016/j.virol.2013.10.006
- Liu Y, Hill MG, Klose T, Chen Z, Watters K, Bochkov YA, et al. Atomic structure of a rhinovirus C, a virus species linked to severe childhood asthma. *Proc Natl Acad Sci*. (2016) 113:8997–90025. doi: 10.1073/pnas.1606595113

47. Simmonds P, McIntyre C, Savolainen-Kopra C, Tapparel C, Mackay IM, Hovi T. Proposals for the classification of human rhinovirus species C into genotypically assigned types. *J Gen Virol.* (2010) 91:2409–19. doi: 10.1099/vir.0.023994-0
48. McIntyre CL, Knowles NJ, Simmonds P. Proposals for the classification of human rhinovirus species A, B and C into genotypically assigned types. *J Gen Virol.* (2013) 94:1791–18065. doi: 10.1099/vir.0.053686-0
49. Chonmaitree T, Trujillo R, Jennings K, Alvarez-Fernandez P, Patel JA, Loeffelholz MJ, et al. Acute otitis media and other complications of viral respiratory infection. *Pediatrics.* (2016) 137:e20153555. doi: 10.1542/peds.2015-3555
50. Sam Narean J, Glanville N, Nunn CM, Niespodziana K, Valenta R, Johnston SL, et al. Epitope mapping of antibodies induced with a conserved rhinovirus protein generating protective anti-rhinovirus immunity. *Vaccine.* (2019) 37:2805–135. doi: 10.1016/j.vaccine.2019.04.018
51. Bochkov YA, Devries M, Tetreault K, Gangnon R, Lee S, Bacharier LB, et al. Rhinoviruses A and C elicit long-lasting antibody responses with limited cross-neutralization. *J Med Virol.* (2023) 95:e29058. doi: 10.1002/jmv.29058
52. Behzadi MA, Choi A, Duehr J, Feyznehzad R, Upadhyay C, Schotsaert M, et al. A cross-reactive mouse monoclonal antibody against rhinovirus mediates phagocytosis *in vitro.* *Sci Rep.* (2020) 10:97505. doi: 10.1038/s41598-020-66600-x
53. Mazanec MB, Kaetzel CS, Lamm ME, Fletcher D, Nedrud JG. Intracellular neutralization of virus by immunoglobulin A antibodies. *Proc Natl Acad Sci.* (1992) 89:6901–5. doi: 10.1073/pnas.89.15.6901
54. Niespodziana K, Napora K, Cabauatan C, Focke-Tejkl M, Keller W, Niederberger V, et al. Misdirected antibody responses against an N-terminal epitope on human rhinovirus VP1 as explanation for recurrent RV infections. *FASEB J.* (2012) 26:1001–85. doi: 10.1096/fj.11-193557
55. Lewis GK, Chu-Pei F. Intrinsic immunogenicity of an internal VP1 T-B epitope pair of type 1 poliovirus. *Mol Immunol.* (1992) 29:1477–855. doi: 10.1016/0161-5890(92)90221-I
56. Cello J, Samuelson A, Stålhandske P, Svennerholm B, Jeansson S, Forsgren M. Identification of group-common linear epitopes in structural and nonstructural proteins of enteroviruses by using synthetic peptides. *J Clin Microbiol.* (1993) 31:911–16. doi: 10.1128/jcm.31.4.911-916.1993
57. Samuelson A, Forsgren M, Johansson B, Wahren B, Sällberg M. Molecular basis for serological cross-reactivity between enteroviruses. *Clin Diagn Lab Immunol.* (1994) 1:336–41. doi: 10.1128/cdli.1.3.336-341.1994
58. Gaido CM, Stone S, Chopra A, Thomas WR, Souëf PNLE, Hales BJ. Immunodominant T-cell epitopes in the VP1 capsid protein of rhinovirus species A and C. *J Virol.* (2016) 90:10459–715. doi: 10.1128/JVI.01701-16
59. Fricks CE, Hogle JM. Cell-induced conformational change in poliovirus: externalization of the amino terminus of VP1 is responsible for liposome binding. *J Virol.* (1990) 64:1934–45. doi: 10.1128/jvi.64.5.1934-1945.1990
60. Lewis JK, Bothner B, Smith TJ, Siuzdak G. Antiviral agent blocks breathing of the common cold virus. *Proc Natl Acad Sci.* (1998) 95:6774–785. doi: 10.1073/pnas.95.12.6774
61. Kolatkar PR, Bella J, Olson NH, Bator CM, Baker TS, Rossmann MG. Structural studies of two rhinovirus serotypes complexed with fragments of their cellular receptor. *EMBO J.* (1999) 18:6249–595. doi: 10.1093/emboj/18.22.6249